BIOCELL
2024 48(2): 313-325

Tech Science Press

Valtrate exerts anticancer effects on gastric cancer AGS cells by regulating reactive oxygen species-mediated signaling pathways

Jinglong CAO[1,#]; Shumei LI[2,#]; Tong ZHANG[1,#]; Jian LIU[1]; Wenshuang HOU[1]; Anqi WANG[1]; Chang WANG[3,4,*]; Chenghao JIN[1,3,5,*]

[1] Department of Biochemistry and Molecular Biology, College of Life Science and Technology, Heilongjiang Bayi Agricultural University, Daqing, 163319, China
[2] Hemodialysis Center, Daqing Oilfield General Hospital, Daqing, 163001, China
[3] Department of Food Science and Engineering, College of Food Science, Heilongjiang Bayi Agricultural University, Daqing, 163319, China
[4] Agricultural Products and Processed Products Supervision and Testing Center, Ministry of Agriculture, Daqing, 163319, China
[5] National Coarse Cereals Engineering Research Center, Daqing, 163319, China

Key words: Valtrate, Gastric cancer cell apoptosis, Cell cycle, Cell migration, Reactive oxygen species

Abstract: Background: Valtrate (Val) was extracted from the *Valeriana jatamansi Jones* plant, had good antitumor activity. However, its precise molecular mechanism in cancer cells was still unclear. This study investigated the effect of Val on gastric cancer (GC) cells and its potential molecular mechanism. **Methods:** Cell viability was examined by CCK-8 assay. Cell cycle, apoptosis, and Reactive oxygen species (ROS) level were analyzed by flow cytometry. The migration effect of Val on AGS cells was analyzed by transwell and wound-healing assay. The expression levels of proteins were analyzed by western blot. **Results:** The cell viability assay results demonstrated that Val significantly decreased GC cell viability. Apoptosis assay results revealed that Val induced mitochondria-dependent apoptosis through the Bad/Bcl-2/cyto-c/cle-casp-3/cle-PARP pathways. Further exploration found that Val induced apoptosis through increasing the expression of phosphorylated p38 mitogen-activated protein kinase (p-p38), phosphorylated c-Jun N-terminal kinase (p-JNK), and Inhibitor kappa B alpha (IκB-α) proteins and decreasing the expression of phosphorylated extracellular signal-regulated kinase (p-ERK), phosphorylated signal transducer and activator of transcription 3 (p-STAT3), and nuclear factor kappa-B (NF-κB) proteins; these expression levels of proteins were reversed by mitogen-activated protein kinase (MAPK) inhibitor. Furthermore, Val induced G2/M phase arrest in AGS cells through downregulating the expression of phosphorylated protein kinase B (p-AKT). Moreover, Val induced inhibition of AGS cell migration through downregulating the expression of p-GSK-3β and β-catenin. In addition, Val promoted the ROS accumulation of AGS cells. Further investigation found that Val-induced apoptosis, arrested the cell cycle, and inhibited cell migration, and that its signaling pathways related to protein expressions were reversed by the ROS scavenger, N-acetyl-L-cysteine. **Conclusion:** Val induced apoptosis, arrested the cell cycle, and inhibited migration by ROS-mediated MAPK/STAT3/NF-κB, AKT/Cyclin B/CDK1/2, and GSK-3β/β-catenin signaling pathways in AGS cells.

Introduction

Gastric cancer (GC) is a global common malignancy and is extremely harmful to human health [1]. The fatality rate of GC is very high, with tens of millions of people dying from the disease each year [2]. Surgery, radiotherapy, and chemotherapy are the three pillars of tumor treatment, but surgery and radiotherapy are only suitable for local treatment, and only a very small percentage of patients survive the first 5 years after therapy [3,4]. While conventional chemotherapy addresses residual cancer cells and decreases recurrence risk, it carries drawbacks like low efficacy, numerous side effects, and a gloomy prognosis [5]. Therefore, the development of high-efficiency and low-toxicity drugs is urgent for GC.

Natural medicine benefits from high-efficacy, low-toxicity, and minimal negative effects and has been highly valued by researchers [6,7]. Valtrate (Val) is the main active component of the medicinal plant *Valeriana jatamansi*

*Address correspondence to: Chang Wang, wangchang@byau.edu.cn; Chenghao Jin, jinchenghao3727@byau.edu.cn
#These authors contributed equally to this work
Received: 03 July 2023; Accepted: 16 October 2023;
Published: 27 February 2024

Doi: 10.32604/biocell.2023.043474

Jones, "The botanical name of the plant material was verified using 'The Plant List website–http://www.theplantlist.org' (accessed on August 25, 2023)". Which has good therapeutic effects on anxiety and depression [8,9]. In addition, Val has exerted good antitumor effects in pancreatic, breast, and ovarian cancer cells by inducing tumor cell apoptosis [10–12]. However, the antitumor activity of Val and its intrinsic molecular mechanism has still received little investigation in treating GC cells.

The dysfunction of cell apoptosis can lead to the occurrence of tumors [13]. Natural drugs induce tumor cell apoptosis and suppress tumor development. Therefore, they have been widely studied by researchers [14–16]. Apoptosis could be induced by a variety of pathways. As the control center of cellular life activities, mitochondria are crucial in regulating apoptosis [17]. In the Bcl-2 family, Bcl-2 and Bad perform opposite functions in the cell apoptosis process [18]. They are the key proteins of mitochondria-mediated apoptosis and can regulate the permeability of the mitochondrial inner membrane and lead to the release of cytochrome c (cyto-c), which is a critical step in apoptosis [19]. The cyto-c can bind to relevant apoptotic factors, activate cleaved-caspase-3 (cle-casp-3) proteins, resulting in a cascade reaction, then cleave substrate PARP (cle-PARP), and lead to cell apoptosis [20].

Reactive oxygen species (ROS) are byproducts of cellular metabolism, which are made up of many oxygen-containing free radicals [21]. ROS are crucial in regulating cell apoptosis and can activate various antitumor signaling pathways such as mitogen-activated protein kinase (MAPK), signal transducer and activator of transcription 3 (STAT3), and nuclear factor kappa-B (NF-κB) [22,23]. Mitogen-activated protein kinase (MAPK) signaling pathways can be activated by various extracellular stimuli, such as oxidative stress, cytokines, and hormones, and can regulate cell proliferation and apoptosis [24]. The signal transducer and activator of transcription 3 (STAT3) signaling pathways are involved in the occurrence, proliferation, and immune evasion of tumor cells [25]. Sustained activation of the nuclear factor kappa B (NF-κB) leads to anti-apoptosis and uncontrolled cell growth [26]. Furthermore, ROS can not only regulate cell apoptosis but can also regulate cell cycle and migration by regulating various signaling pathways [27,28].

The process by which a cell advances from the end of its first division to the end of its second division is known as the cell cycle [29]. The process is tightly regulated by many signaling pathways and proteins [30]. If the signaling pathway in this process is abnormally regulated, uncontrolled cell division may occur, eventually leading to tumorigenesis [31]. The protein kinase B (AKT) signaling pathway, as a proto-oncogene, is crucial in tumor cell cycle regulation and can regulate cell cyclin-related proteins expression necessary to arrest the tumor cell cycle and reduce proliferation [32].

Tumor cell migration can cause tumors to spread and make tumor treatment more difficult [33]. The inhibition of tumor cell migration has become an active research topic regarding tumor treatment [34]. Glycogen synthase kinase 3β (GSK-3β) is a downstream protein of the AKT signaling pathway that is essential for the development and growth of tumors [35]. Inhibiting GSK-3β, a factor that promotes cancer, would promote β-catenin to enter the nucleus, activate the β-catenin signaling pathway, and finally inhibit tumor cell migration [36].

In this study, the effects of Val on AGS cell apoptosis, cell cycle arrest, and inhibition of migration, as well as their molecular mechanisms were investigated.

Materials and Methods

Reagents

Val and 5-FU were obtained from Sigma-Aldrich (St. Louis, MO, USA). After calculating the mass of the required compound and the volume of 100% dimethyl sulfoxide (DMSO, Solarbio, Beijing, China), the DMSO and the compound were stirred and dissolved at 37°C aseptic condition to prepare a 20 mM stock solution and stored at −20°C.

Cell culture

Twelve types of GC cells (AGS, NCI-N87, YCC-6, SNU-484, KATO-3, YCC-16, YCC-1, MKN-45, SNU-668, SNU-5, MKN-28, and SNU-216) and human embryonic lung fibroblasts (IMR-90) were obtained from the American Type Culture Collection (Manassas, VA, USA). Human normal gastric cells (GES-1), human liver immortalized cells (THLE-2), and human embryonic kidney cells (293T) were purchased from Saiqi Biotech Co., Ltd. (Shanghai, China). Cells were cultured in an incubator with 5% CO_2 and 37°C using RPMI 1640 medium (Gibco, Waltham, USA) or Dulbecco's modified eagle medium (DMEM, Gibco) that contains 10% fetal bovine serum (FBS, Gibco) and 1% penicillin/streptomycin (P/S, Gibco). Logarithmic growth phase cells were obtained and used in the experiment. The cell density reached 80% to passage cells grown.

Cell viability assay

Ninety-six-well plates were seeded with twelve types of GC cells and four types of normal cells (1×10^4 cells/well). Val and 5-FU were treated at different concentrations for 24 h. Cells were cultured in 10 μL of CCK-8 solution (Solarbio) for 3 h without exposure to light. Cell viability was measured using a microplate luminometer (BioTek Instruments, Inc., VT, USA). The IC_{50} value was determined using the GraphPad Prism 5.0 program. In addition, Val and 5-FU, in accordance with their respective IC_{50} values, treated cells for 0, 6, 12, 18, 24, and 30 h, and the survival rates of each kind of cell were examined.

Cell apoptosis assay

Six-well plates were seeded with AGS cells (1×10^5 cells/well). Val (30 μM, IC_{50} value) was treated for 3, 6, 12, and 24 h. The apoptotic effect of Val on AGS cells was analyzed using Annexin V-FITC Apoptosis Detection Kits (Solarbio). AGS cells were stained with 4 μL of Annexin V-FITC and 2 μL of propidium iodide (PI) in each well, then placed in the dark for 15 min. After this morphology, the intensity of fluorescence and apoptotic rate of the AGS cells were analyzed using an inverted microscope (Mingmei

Optoelectronics Co., Guangzhou, China) and flow cytometry (Sysmex Co., Kobe, Japan).

A drop in mitochondrial membrane potential (MMP) accompanied the apoptotic process. The MMP effect of Val on AGS cells was analyzed using JC-1 Kit (Solarbio). 500 μL 1 × JC-1 working solution stained AGS cells for 30 min at 37°C. Then 500 μL pre-cooled 1 × washing buffer washed away excess JC-1. The change in MMP was determined with flow cytometry.

Western blot analysis

The lysis buffer was mixed with the collected cells for 30 min to make a protein sample. Then, 8–12% SDS-PAGE gel electrophoresis was performed to fractionate proteins, and proteins were then transferred to nitrocellulose membranes. Which was then incubated in 5% skim milk for 2 h. Primary antibodies of α-tubulin, Bad, STAT3, p-STAT3, cle-casp-3, cle-PARP, p-GSK-3β, AKT, p38, p-p38, E-cadherin, Bcl-2, IκB-α, NF-κB, β-catenin, GSK-3β, p-AKT, ERK, p-ERK, Cyclin B, CDK1/2, N-cadherin, JNK, p-JNK, p21, p27, IL-6, and cyto-c (Santa Cruz Biotechnology, Inc., Dallas, USA) were added and incubated overnight at 4°C. After that, secondary antibodies of anti-mouse and anti-rabbit (ZSGB-Bio, Inc., Beijing, China) were added and incubated for 2 h. Finally, proteins were visualized using an enhanced chemiluminescnce kit (Tanon, Shanghai, China) and UVP ChemStudio 515 (Schisen Micron Medical Electronics Co., Ltd., Shanghai, China).

ROS level assay

Six cm plates were seeded with AGS cells (1×10^6 cells/plate). After Val (30 μM) treatment, AGS cells were stained by DCFH-DA probe according to the ROS detection kit (Beyotime Institute Biotechnology, Shanghai, China) for 30 min at 37°C. Finally, accumulations of ROS in AGS cells were analyzed with flow cytometry.

Cell cycle assay

Six cm plates were seeded with AGS cells (1×10^6 cells/plate). Val (30 μM) was treated for 3, 6, 12, and 24 h. The cells were treated with 70% alcohol at 4°C for 4 h. A quantity of 100 μL RNase A (10 μg/mL) treated cells at 37°C for 30 min, after which 400 μL PI (10 μg/mL) was added to stain AGS cells for 20 min. Finally, the cell cycle was analyzed with flow cytometry.

Cell migration assay

Six-well plates were seeded with AGS cells (1×10^5 cells/well). When the cells reached 90% density, the tip of a 200 μL sterile pipette was used to draw a line of equal width to form a scratch. Then, the cells were treated with a medium containing Val, and photographs of the scratch were taken with an inverted microscope at 3, 6, 12, and 24 h. The image analysis software "ImageJ" was used to measure and analyze the scratch width at each time point. The "line tool" was used to draw a line on each side of the scratch, and click "Analyze" > "Measure" to take the measurement and record the width of the scratch. In the transwell assay, AGS cells (1×10^5) were added to the upper chamber of the twenty-four-well transwell plates, and the medium did not contain FBS. Medium containing 10% FBS was added to the lower chamber, then placed in an incubator at 37°C and 5% CO_2 for incubation (3, 6, 12, and 24 h). After incubation at each time point, and the cells in the lower chamber were then stained with 0.1% crystal violet (Solarbio) for 10-20 min and recorded by inverted microscope. Then, cell counts were performed using ImageJ software. After selecting area, "Image" > "Adjust" > "Threshold", adjust the threshold so that the cell area is black and the background is white, click "Analyze" > "Analyze Particles", then click "OK" to analyze the count of cells.

Statistical analysis

All the data are expressed as the mean ± standard deviation (SD) and were presented as a mean of three independent experiments. The cell migration was analyzed by the ImageJ software. The IC_{50} was calculated by SigmaPlot 15.0 software. SPSS 29.0 software was used to perform Tukey's *post hoc* test; multiple comparisons across the groups were conducted using a one-way analysis of variance. A p value of <0.05 was regarded as significant.

Results

Val exhibits the cytotoxic effect in GC cells

To determine whether Val can inhibit the viability of GC cells, the viability of cells was determined by CCK-8 assay. It found that Val significantly inhibited the viability of twelve types of GC cells in a dose-dependent and time-dependent manner, and the inhibitory effects of Val on the viability of GC cells were much higher than that of 5-FU (Figs. 1A and 1B). Table 1 displays the Val and 5-FU IC_{50} values for each GC cell. To determine whether Val has a toxic side effect on normal cells, four types of normal cells (IMR-90, 293T, THLE-2, and GES-1) viability was determined by CCK-8 assay. It was found that Val did not clearly have a cytotoxic effect on normal cells, and the cytotoxic effect of Val on normal cells was significantly lower than that of 5-FU (Figs. 1C and 1D).

Val induces apoptosis in AGS cells

To verify whether the cytotoxic effect of Val on AGS cells was associated with apoptosis, Annexin V-FITC and PI double staining assay was performed. The results showed that Val treatment exhibited significantly more fluorescence in the AGS cells than the 5-FU group, and the fluorescence intensity increased over time (Fig. 2A). The flow cytometry results showed that the sum of the proportion of early and late apoptosis induced by Val at 24 h significantly increased to 40.45% compared with the untreated group (Fig. 2B). Additionally, early apoptotic cells were accompanied by changes in MMP. Val treatment reduced the MMP to 24% at 24 h, which was the main characteristic feature of early apoptosis (Fig. 2C). Further protein level analysis revealed that Val treatment up-regulated Bad, cyto-c, cle-casp-3, and cle-PARP expression and down-regulated Bcl-2 expression (Fig. 2D).

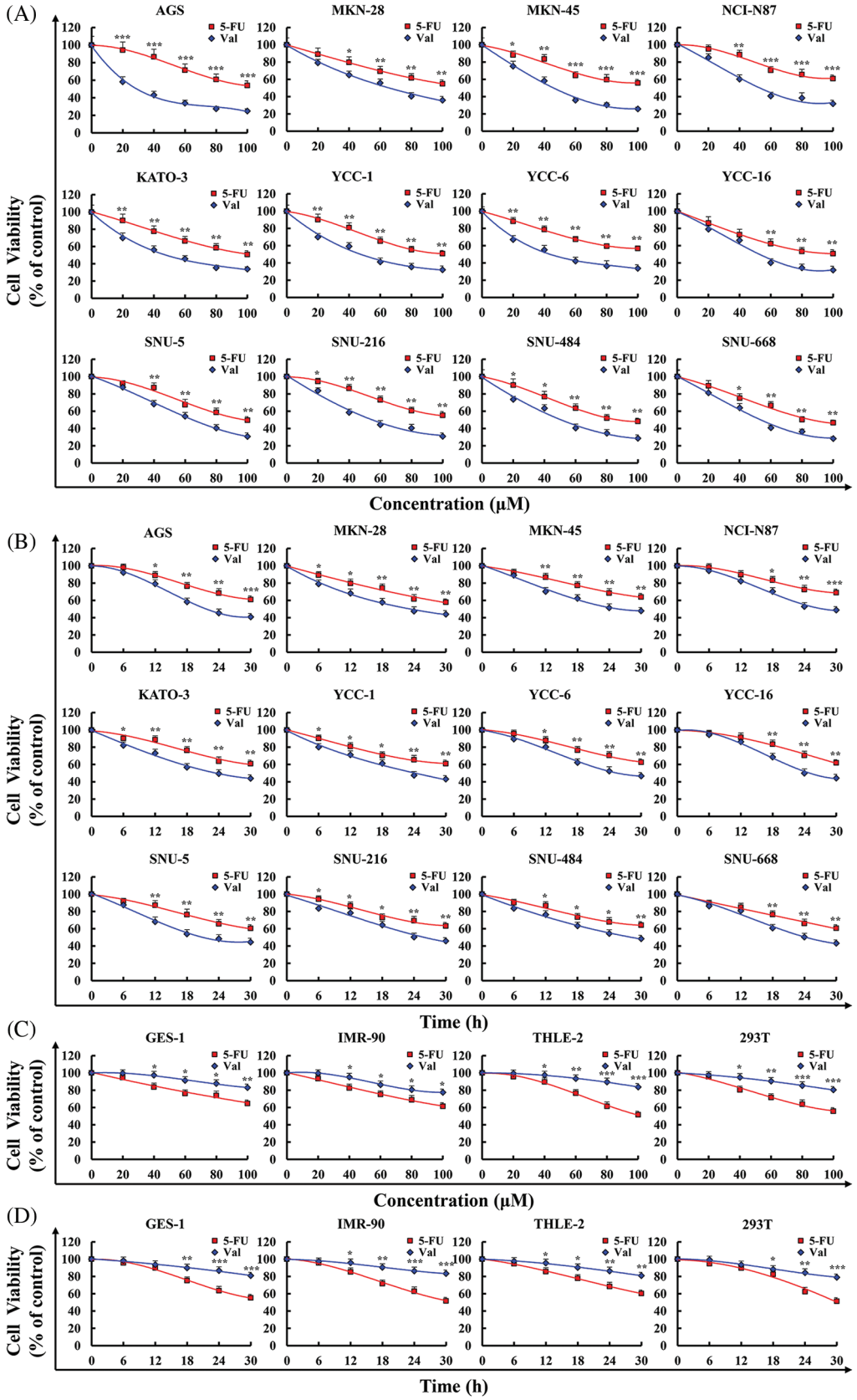

FIGURE 1. The cytotoxic effects of Val in GC cells. (A) Cells were treated with various concentrations of 5-FU or Val (20, 40, 60, 80, and 100 μM) for 24 h. Viability of twelve types of GC cells were detected using CCK-8 assay. (B) Cells were treated with 5-FU and Val IC_{50} concentrations for various times (6, 12, 18, 24, and 30 h). Viability of twelve types of GC cells were detected using CCK-8 assay. (C) Cells were treated with various concentrations of 5-FU or Val (20, 40, 60, 80, and 100 μM) for 24 h. Viability of four types of normal cells were detected using CCK-8 assay. (D) Cells were treated with 5-FU and Val IC_{50} concentrations for various times (6, 12, 18, 24, and 30 h). Viability of four types of normal cells were detected using CCK-8 assay. $^{*}p < 0.05$, $^{**}p < 0.01$ and $^{***}p < 0.001$ *vs.* 5-FU.

TABLE 1

IC_{50} values of Val and 5-FU in GC cells

Cell line	5-FU (μM)	Val (μM)
AGS	104 ± 3.45	30 ± 2.32
MKN-28	103 ± 2.37	67 ± 3.51
MKN-45	106 ± 3.35	45 ± 2.65
NCI-N87	112 ± 2.86	54 ± 2.76
KATO-3	99 ± 3.41	49 ± 3.27
YCC-1	97 ± 2.89	52 ± 3.35
YCC-6	105 ± 3.64	43 ± 2.69
YCC-16	100 ± 3.12	48 ± 3.22
SNU-5	98 ± 2.76	63 ± 2.75
SNU-216	103 ± 3.37	57 ± 3.24
SNU-484	94 ± 2.52	51 ± 2.65
SNU-668	96 ± 3.45	50 ± 3.08

Val induces AGS cell apoptosis through the MAPK/STAT3/NF-κB signaling pathways

To further investigate the molecular mechanisms responsible for the Val-induced apoptosis of AGS cells, the expression levels of MAPK/STAT3/NF-κB signaling pathway-related proteins were detected by western blot. And found that after Val-treated AGS cells, p-p38, p-JNK, and IκB-α expression obviously increased, whereas p-ERK, p-STAT3, IL-6, and NF-κB expression obviously decreased (Fig. 3A). In order to verify the interaction and influence between MAPK and STAT3 signaling pathways, the expression of p-STAT3 protein was detected by western blot after MAPK inhibitor pretreatment, and the results showed that the inhibitory effect of Val on the expression of p-STAT3 protein was enhanced in the Val + ERK inhibitor (FR180204) treatment group. The inhibitory effect of Val on the expression of p-STAT3 protein was weakened in the Val + JNK inhibitor (SP600125) treatment group and Val + p38 (SB203580) inhibitor treatment group (Figs. 3B–3D).

Val induces AGS cell apoptosis via ROS-mediated MAPK/STAT3/NF-κB signaling pathways

To investigate whether ROS are related to Val-induced apoptosis, intracellular ROS level were detected by flow cytometry and it found that treatment of AGS cells with Val resulted in a gradually increase in intracellular ROS accumulation over time (Fig. 4A). The accumulation of ROS was decreased in GES-1 cells by Val (Fig. 4B). N-acetyl-L-cysteine (NAC) is a commonly used antioxidant. The regulatory role of ROS in Val-induced apoptosis of AGS cells was further detected by NAC pretreatment. The results showed that the summation of the ratio of early and late apoptosis of the Val + NAC group was severely reduced when compared to the Val alone treatment group (down from 39.86% to 22.94%) (Fig. 4C). The inhibition of p-ERK, p-STAT3, and NF-κB expression and the promotion of p-p38, p-JNK, IκB-α, cle-casp-3, and cle-PARP expression regulated by Val were reversed in the Val + NAC group (Fig. 4D).

Val induces G2/M phase arrest in AGS cells

To investigate whether apoptotic cells induced by Val affected the cell cycle, the cell cycle was detected by flow cytometry, and the results showed that after Val treatment, the proportion of cells in the G1 phase gradually decreased from 53.34% to 34.83%, and the G2/M phase gradually increased from 5.69% to 20.61% (Fig. 5A). To verify whether ROS accumulation is involved in cell cycle regulation, cell cycle distribution and cycle-related proteins were further detected by NAC pretreatment in AGS cells. The results showed that the percentage of G2/M phase cells of the Val + NAC group was significantly decreased to 15.51%, which was significantly lower than that in the Val alone treatment group (Fig. 5B). Subsequently, western blot analysis results showed that Val treatment increased p21 and p27 expression, while p-AKT, CDK1/2, and Cyclin B had the opposite effect (Fig. 5C). The inhibition of p-AKT, Cyclin B, and CDK1/2 protein expression and the promotion of p21 and p27 expression regulated by Val were reversed in the Val + NAC group (Fig. 5D).

Val inhibits AGS cell migration

To investigate whether Val could inhibit AGS cell migration and invasion, the effect of Val on AGS cell migration was detected by wound-healing and transwell assay. And it found that significantly fewer cells migrated when comparing the Val group to the control group, and the inhibitory effect became more apparent after 6 h (Fig. 6A). In comparison to the control group, the wound-healing trend in the Val group was severely hampered (Fig. 6B). To verify whether ROS accumulation is involved in the regulation of AGS cell migration, cell migration was further detected by NAC pretreatment, and found that the wound-healing rate of the AGS cells in the Val + NAC group was significantly increased compared with that of the Val alone group (Fig. 6C). The expression of migration-related proteins was further examined and Val treatment increased E-cadherin expression and decreased p-AKT, p-GSK-3β, β-catenin, and N-cadherin expression (Fig. 6D). In the Val + NAC group, Val-regulated p-AKT, p-GSK-3β, β-catenin, N-cadherin, and E-cadherin expression were reversed (Fig. 6E).

Discussion

As a common drug in chemotherapy, 5-FU has made some progress in the process of tumor treatment, but the adverse effects caused by its toxic side effects are difficult to overcome [37]. Some studies have shown that natural drug extracts have good antitumor effects and have the advantages of low toxicity and high efficiency; therefore, they have become a new choice for tumor treatment [38,39]. This study confirmed that Val has a cytotoxic effect on GC cells, is significantly more effective than 5-FU, and has lower toxicity on four types of normal cells. GC cells showed different sensitivity to Val, which we speculated might be due to the different cellular metabolites and drug sensitivity of GC cells from different sources [40]. AGS cells were the most sensitive to Val treatment, so AGS cells were used as the experimental subjects in the subsequent

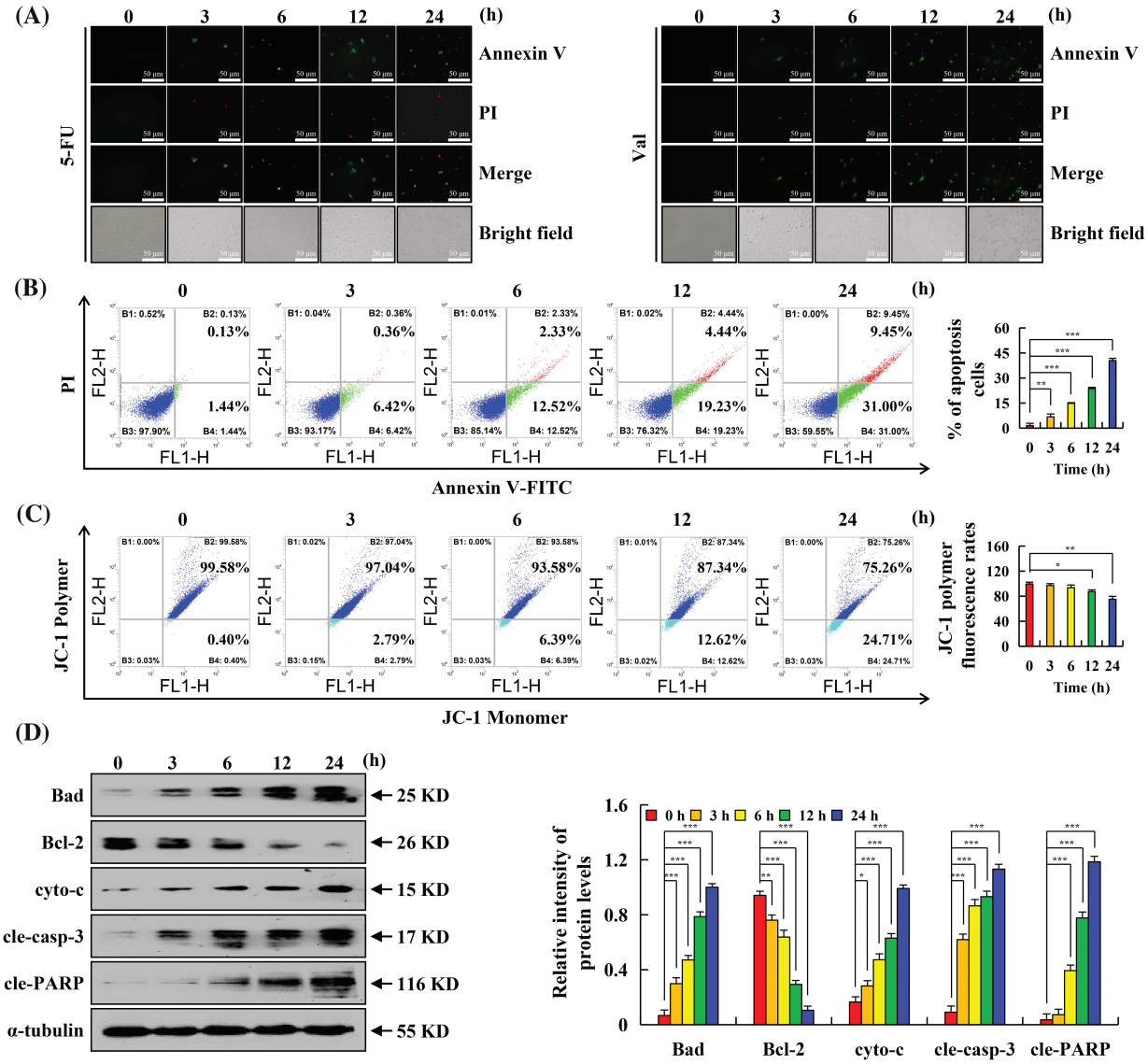

FIGURE 2. The apoptotic effects of Val in AGS cells. AGS cells treated with 30 μM Val for various times (3, 6, 12, and 24 h). (A) AGS cells were stained with Annexin V-FITC/PI, and cell morphology was observed using a fluorescence microscope (original magnification is 400×). (B) AGS cells were stained with Annexin V-FITC/PI, and the apoptotic rate of cells was analyzed with flow cytometry. (C) AGS cells were stained with JC-1, and the MMP of cells was analyzed with flow cytometry. (D) Expression levels of apoptosis-related proteins in AGS cells were analyzed using western blot analysis. α-tubulin was used as an internal reference protein. $^{*}p < 0.05$, $^{**}p < 0.01$ and $^{***}p < 0.001$ *vs*. 0 h.

experiments. Subsequently, we further investigated the antitumor molecular mechanism of Val on AGS cells.

Inducing apoptosis of tumor cells was one of the methods to inhibit tumors [41]. Studies have shown that Bad and Bcl-2 could regulate the release of cyto-c and then generate a caspase cascade to regulate mitochondria-dependent apoptosis [42,43]. In this study, we found that Val could induce apoptosis through the Bcl-2 family pathway. In addition, we found that when the cells were treated for more than 24 h, a large number of AGS cells would be shed, which was not conducive to the continuation of the experiment, so we chose 24 h as the final treatment time point. One study showed that Val could regulate pancreatic cancer cell apoptosis by inhibiting STAT3 activity [10]. Indeed, the STAT3 signaling pathway was also involved in the process of Val-induced apoptosis of AGS cells. We further found that the MAPK and NF-κB signaling pathways were also involved in Val-induced apoptosis, and the MAPK signaling pathway was located upstream of the STAT3 signaling pathway for regulation by MAPK inhibitors treatment experiments. Studies have shown that IL-6, as a cytokine, can activate the IL-6 receptor on the cell surface, and then activate receptor-related JAK enzymes (including JAK1 and JAK2), and phosphorylated JAK enzymes can further activate STAT3 protein, and then regulate the expression of a series of genes [44,45]. In this study, we found that the expression of IL-6 was significantly decreased after Val treatment, and we speculated that Val could also regulate the STAT3 signaling pathway by inhibiting the expression of IL-6 and thus inhibiting the activation of JAK enzyme.

It is well known that tumor cells have higher levels of ROS than normal cells and that excessive ROS in tumor cells has a killing effect on tumor cells [46,47]. Studies have revealed that some natural drugs could exert antitumor

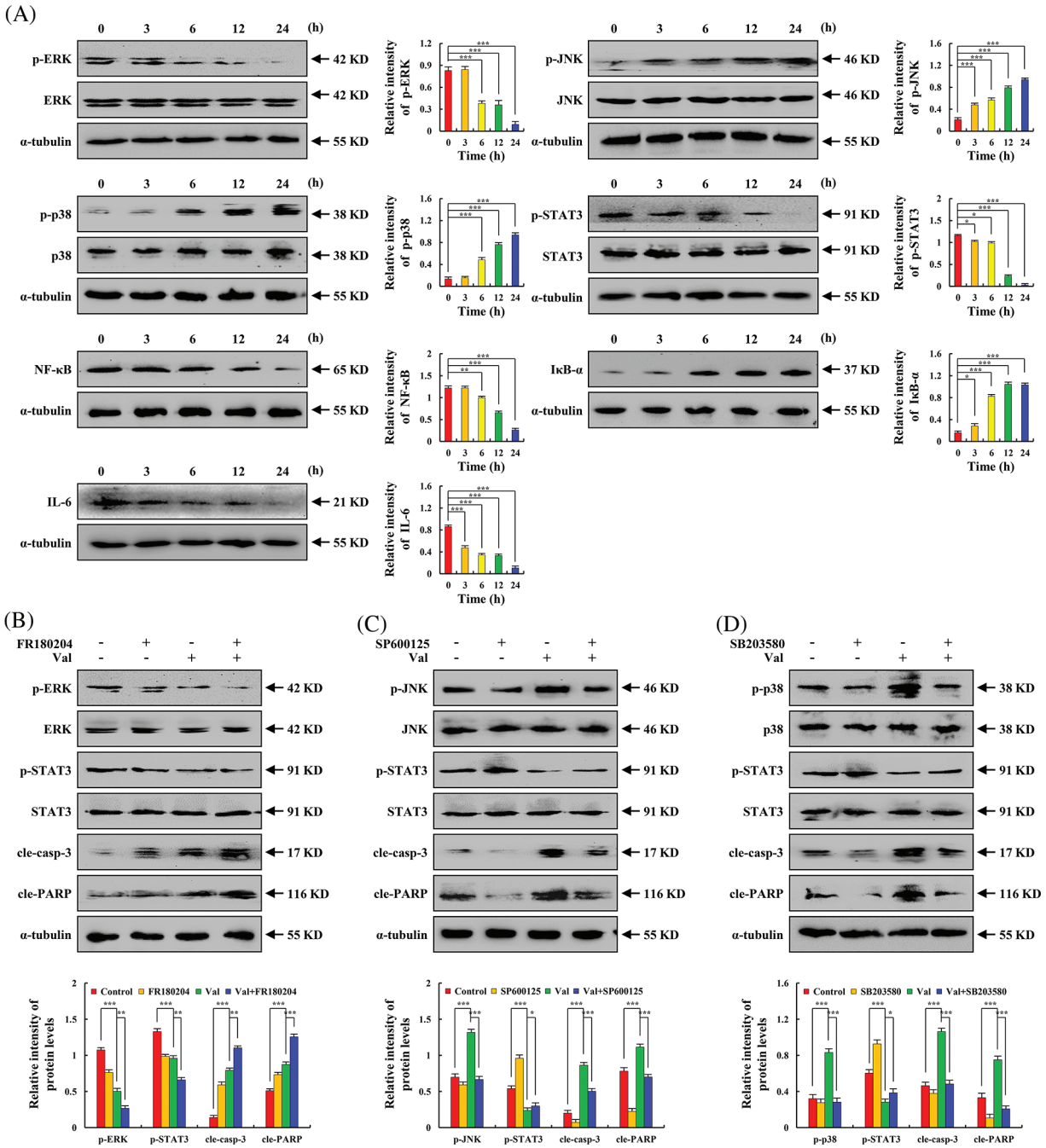

FIGURE 3. The regulatory effects of Val on MAPK, STAT3, and NF-κB signaling pathways in AGS cells. AGS cells were treated with 30 μM Val for various times (3, 6, 12, and 24 h). (A) Expression levels of p-ERK, p-JNK, p-p38, p-STAT3, NF-κB, IL-6, and IκB-α proteins were analyzed using western blot analysis. α-tubulin was used as an internal reference protein. *$p < 0.05$, **$p < 0.01$ and ***$p < 0.001$ *vs.* 0 h. AGS cells were treated with 30 μM Val and/or 10 μM MAPK inhibitors (FR180204, SP600125, and SB203580) for 24 h. (B) Expression levels of p-ERK, p-STAT3, cle-casp-3, and cle-PARP proteins were analyzed using western blot analysis. (C) Expression levels of p-JNK, p-STAT3, cle-casp-3, and cle-PARP proteins were analyzed using western blot analysis. (D) Expression levels of p-p38, p-STAT3, cle-casp-3, and cle-PARP proteins were analyzed using western blot analysis. α-tubulin was used as an internal reference protein. *$p < 0.05$, **$p < 0.01$ and ***$p < 0.001$ *vs.* control or Val + MAPK inhibitor groups.

effects by increasing ROS accumulation [48–50]. To verify whether Val induced ROS accumulation in AGS cells, we detected ROS levels and found that Val could increase ROS accumulation in AGS cells. We further found that Val promotes ROS accumulation and then regulates MAPK, STAT3, NF-κB signaling pathways, and then induces cell apoptosis by ROS inhibitor (NAC) treatment experiments. Interestingly, the role of Val in promoting ROS accumulation in tumor cells was opposite to that in normal human gastric cells. The difference in results may be due to the different metabolic pathways of cancer cells and normal cells and the antioxidant defense mechanisms of cancer cells may be altered. We speculated that Val may increase ROS accumulation by increasing ROS production in cancer cells or reducing their antioxidant defenses. In normal cells, Val may reduce ROS accumulation by enhancing antioxidant

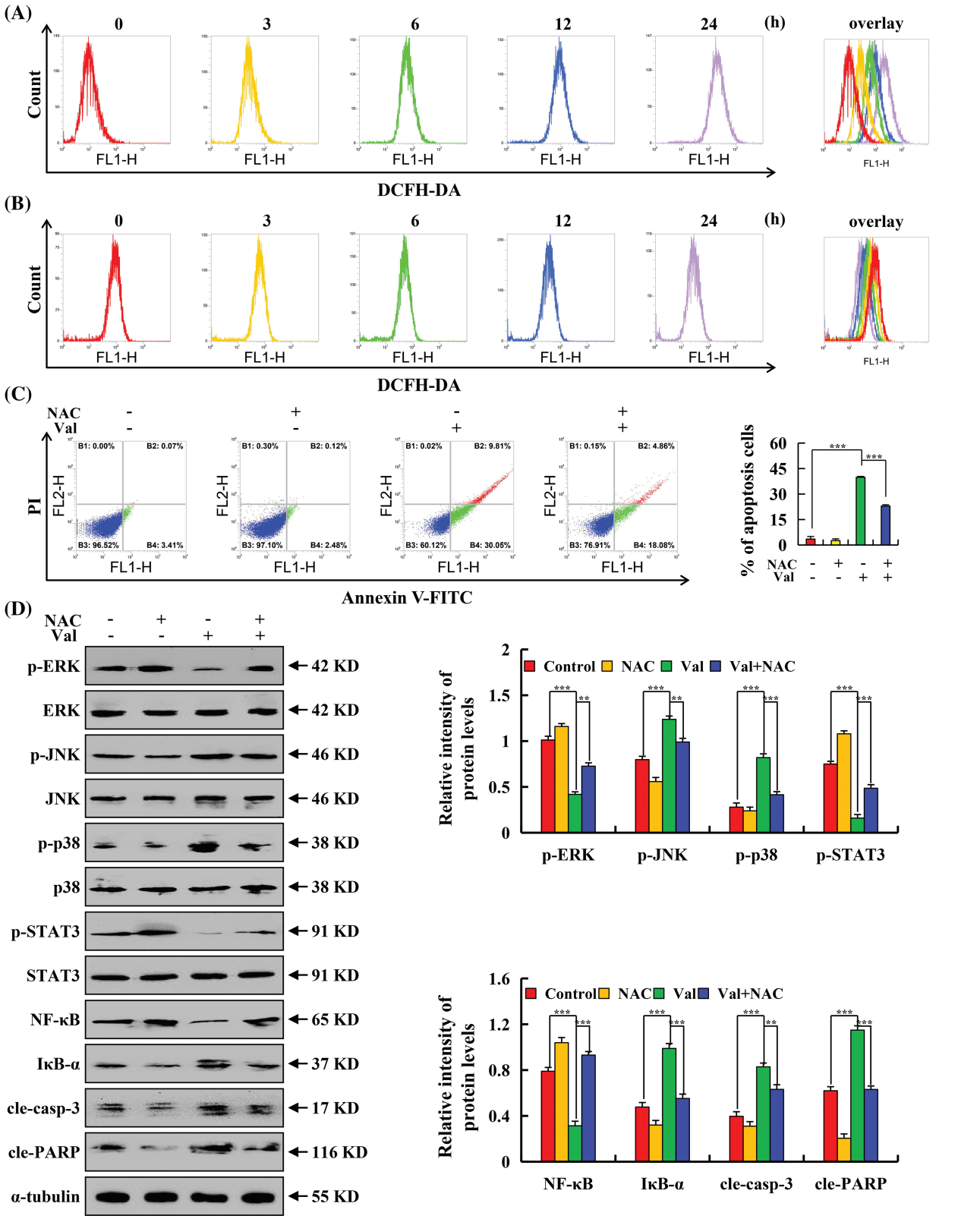

FIGURE 4. The promoting effects of Val on ROS accumulation in AGS cells. AGS cells were treated with 30 μM Val for various times (3, 6, 12, and 24 h). The ROS levels of AGS cells treated by Val at different time points were distinguished by different colors, and then the ROS levels at each time points were overlay for analysis. (A) Intracellular ROS level were analyzed with flow cytometry in AGS cells. (B) Intracellular ROS level were analyzed with flow cytometry in GES-1 cells. AGS cells were treated with 30 μM Val and/or 10 mM NAC for 24 h. (C) The apoptotic rate of AGS cells was analyzed with flow cytometry. (D) Expression levels of p-ERK, p-JNK, p-p38, p-STAT3, NF-κB, IκB-α, cle-casp-3, and cle-PARP proteins were analyzed using western blot analysis. α-tubulin was used as an internal reference protein. $^{*}p < 0.05$, $^{**}p < 0.01$ and $^{***}p < 0.001$ *vs.* control or Val + NAC groups.

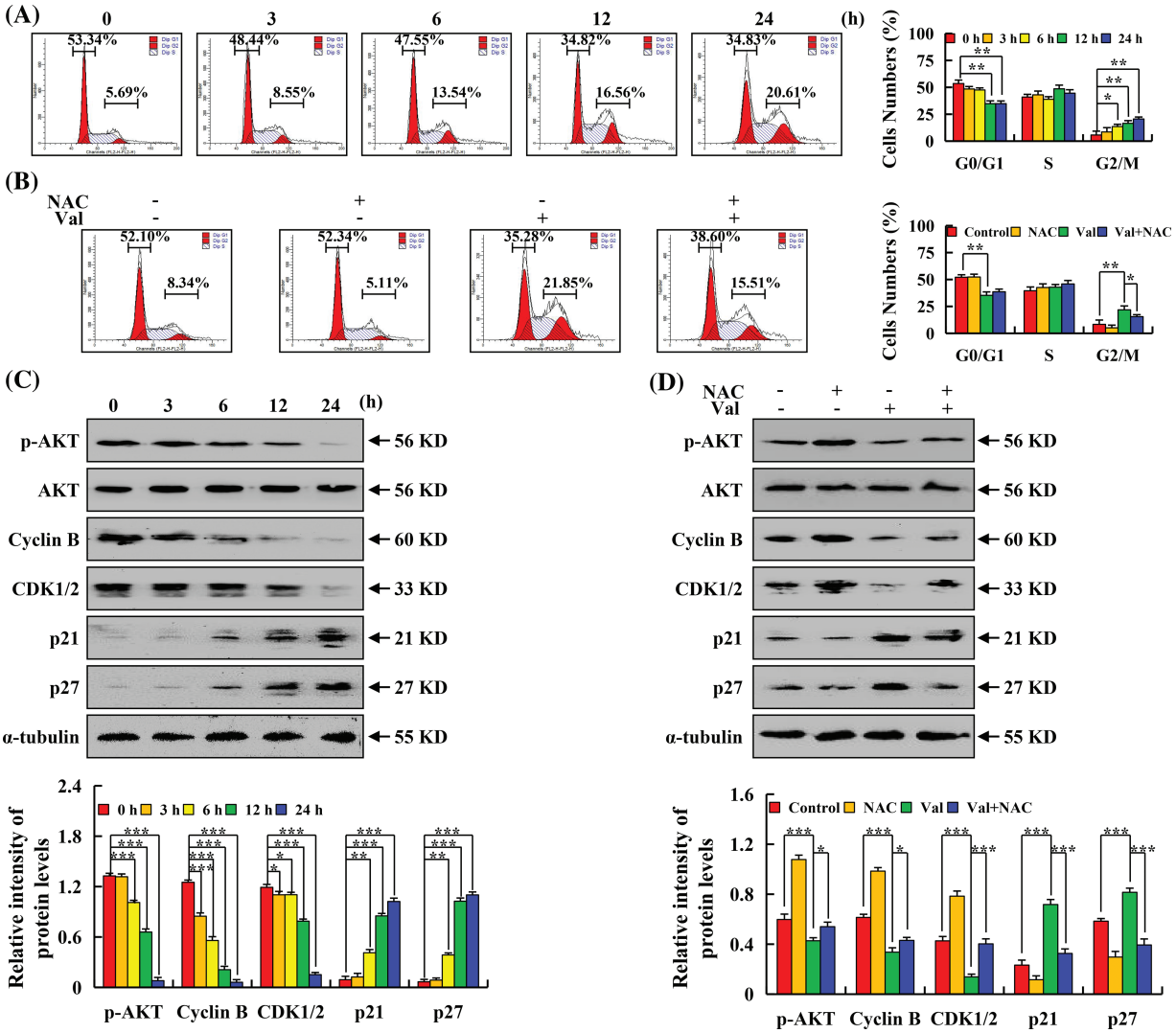

FIGURE 5. The arresting effects of Val on the cell cycle in AGS cells. (A) AGS cells were treated with 30 μM Val for various times (3, 6, 12, and 24 h). The percentage of cell cycle numbers was analyzed with flow cytometry. (B) AGS cells were treated with 30 μM Val and/or 10 mM NAC for 24 h. The percentage of cell cycle numbers was analyzed with flow cytometry. (C) AGS cells were treated with 30 μM Val for various times (3, 6, 12, and 24 h). Expression levels of the G2/M phase cell cycle-related proteins were analyzed using western blot analysis. α-tubulin was used as internal reference protein. $^{*}p < 0.05$, $^{**}p < 0.01$ and $^{***}p < 0.001$ *vs.* 0 h. (D) AGS cells were treated with 30 μM Val and/or 10 mM NAC for 24 h. Expression levels of the G2/M phase cell cycle-related proteins were analyzed using western blot analysis. α-tubulin was used as an internal reference protein. $^{*}p < 0.05$, $^{**}p < 0.01$ and $^{***}p < 0.001$ *vs.* control or Val + NAC groups.

defense mechanisms or reducing ROS production. However, the current limitation is that the biochemistry and molecular processes of cancer cells and normal cells are very complex and may involve many different factors and mechanisms, so it is difficult to determine through which mechanisms Val exerts this effect, and the experimental conditions may not fully mimic the environment in the human body, and the results may not fully reflect what happens in the human body.

Arresting the tumor cell cycle was the main means to prevent the growth of tumor cells [51]. In different cycle stages, corresponding CDK proteins would appear to bind to corresponding cyclin proteins, which then regulate the cycle [52]. To investigate whether Val-induced apoptosis was related to the cell cycle, cell cycle checkpoints and cyclin-related protein expressions were examined. We found that Val induced AGS cell G2/M phase arrest and affected the expression of related proteins in the G2/M phase. The cell cycle arrest was also regulated by ROS. Research has shown that if DNA damaged in cell cycle arrest is not repaired, it could lead to apoptosis of tumor cells [53]. We validated that Val could not only induce apoptosis directly but also induce apoptosis by cell cycle arrest. Meanwhile, we found that the degree of Val to cycle arrest was different in different tumor cells, which might be due to the different DNA repair capacities of different cells [54]. Currently, DNA damage induced by drugs combined with other therapies to kill malignant cells has become a focus of intense study in the tumor treatment field [55]. To contribute more effectively to the usage of combination therapy with Val in the future, the different DNA damage effects of Val in different tumor cells should be considered in further studies.

The treatment of tumors is greatly hampered by the migration of tumor cells [56]. One study has shown that Val could inhibit migration by regulating MMP-2 and MMP-9

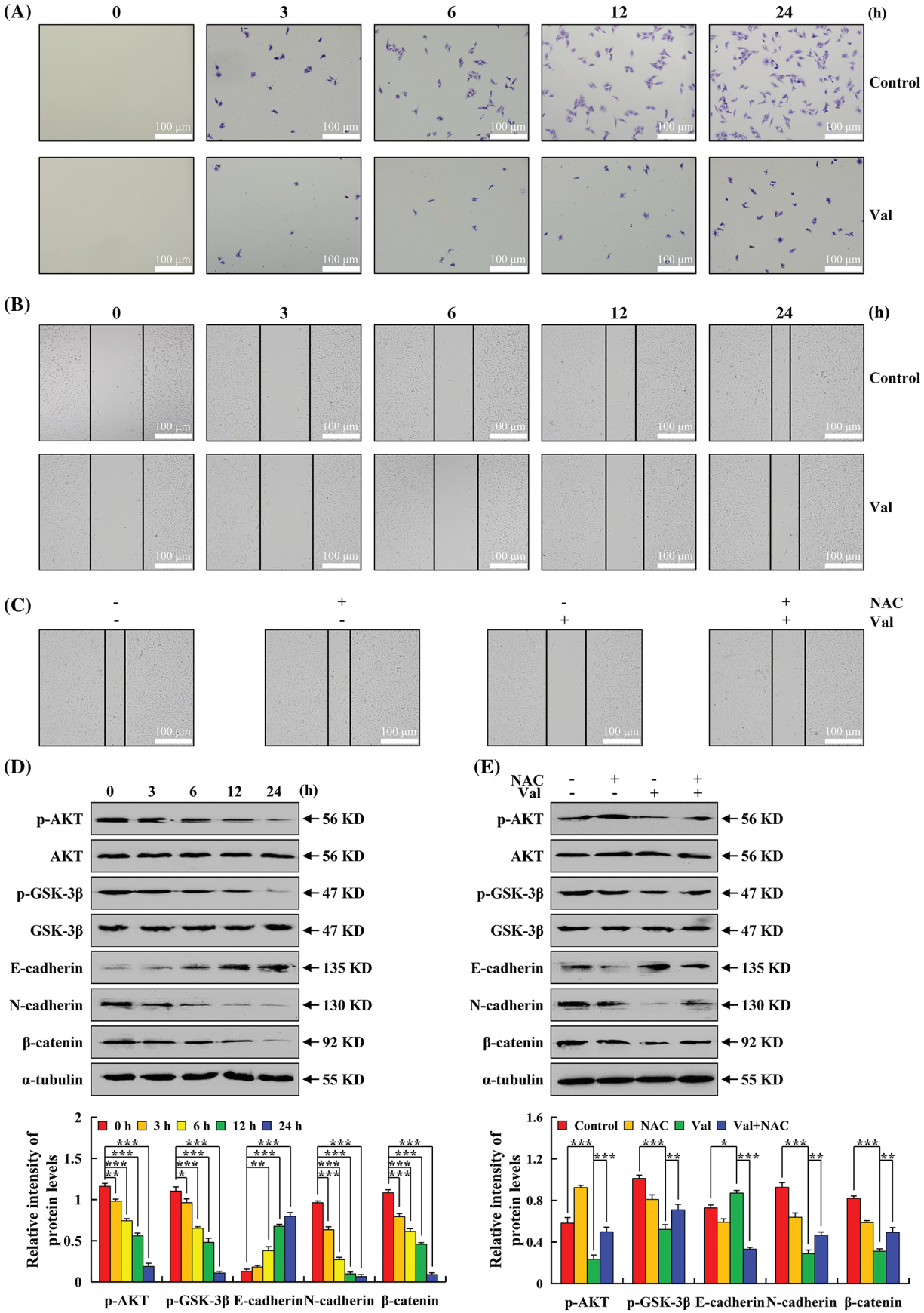

FIGURE 6. The inhibitory effects of Val on cell migration in AGS cells. AGS cells were treated with 30 μM Val for various times (3, 6, 12, and 24 h), and cell migration was analyzed using an inverted microscope (original magnification is 100×). (A) Cell migration was analyzed using transwell assay. (B) Cell migration was analyzed using wound-healing assay. (C) AGS cells were treated with 30 μM Val and/or 10 mM NAC for 24 h. Cell migration was analyzed using wound-healing assay. (D) Cell migration-related proteins were detected using western blot analysis. α-tubulin was used as an internal reference protein. $^{*}p < 0.05$, $^{**}p < 0.01$ and $^{***}p < 0.001$ *vs.* 0 h. (E) AGS cells were treated with 30 μM Val and/or 10 mM NAC for 24 h. Expression levels of cell migration-related proteins were analyzed using western blot analysis. α-tubulin was used as an internal reference protein. $^{*}p < 0.05$, $^{**}p < 0.01$ and $^{***}p < 0.001$ *vs.* 0 h, control, or Val + NAC groups.

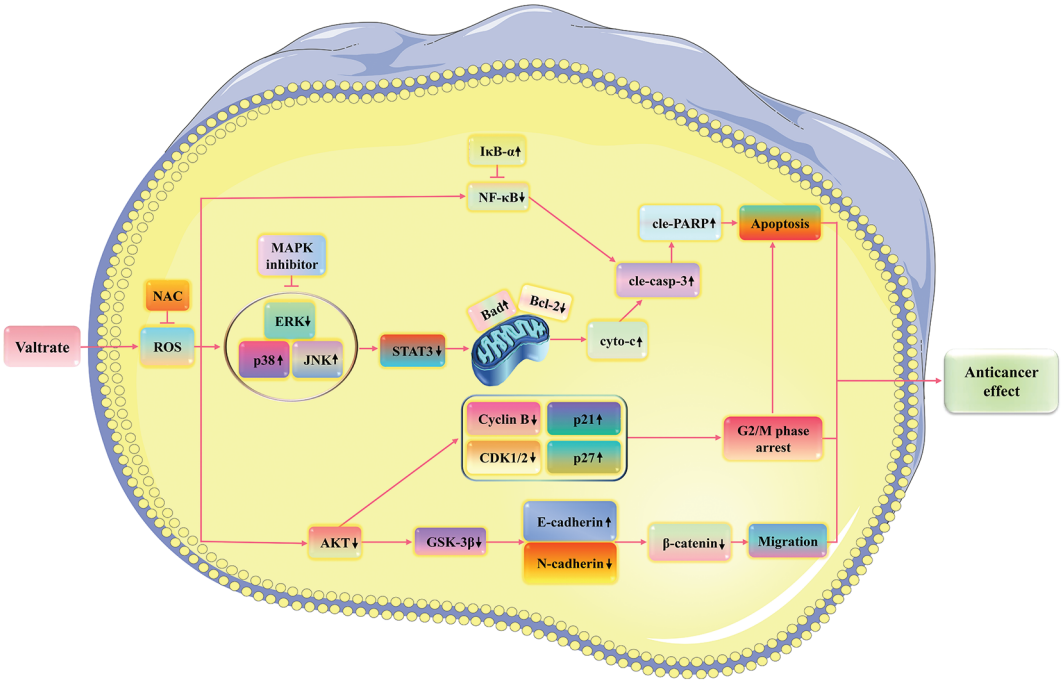

FIGURE 7. Schematic of the signaling pathway of Val in AGS cells. Val exerts good anticancer effects by inducing cell apoptosis, arresting cell cycle, and inhibiting cell migration via ROS-mediated MAPK/STAT3/NF-κB, AKT/Cyclin B/CDK1/2, and GSK-3β/β-catenin signaling pathways.

expression [11]. To verify whether the antitumor effects of Val were associated with the inhibition of migration, the migration ratio of AGS cells and their related pathway protein expression were examined. We found that Val could inhibit migration via the AKT/GSK-3β/β-catenin signaling pathways in AGS cells. Further studies demonstrated that the Val-induced inhibition of migration was regulated by ROS. These results identify the underlying molecular mechanism by which Val inhibited migration, which might be a target for the inhibition of tumor migration in the future. Although our study demonstrated that Val inhibits cell migration by the AKT/GSK-3β/β-catenin signaling pathways, there are still limitations to our study, such as we did not examine the target genes of β-catenin that control cell migration. Detection of this target gene can provide a more detailed understanding of the molecular mechanism by which Val inhibits cell migration. In future studies, we will consider studying these target genes to further elucidate the role of Val in cell migration.

Our study demonstrated that Val induced apoptosis, arrested the cell cycle, and inhibited migration through ROS-mediated MAPK signaling pathways in AGS cells (Fig. 7). Val has shown good anti-GC efficacy with very low toxicity and side effects and has the potential to be a future therapeutic agent for GC. Although our study reveals the anti-cancer mechanism of Val on GC cells, there are still some limitations. Our study focused mainly on GC cells, but the effects of Val on normal cells were not studied in depth. This could affect our overall understanding of the mechanism of action of Val, as there may be differences in how the Val acts on cancer cells and normal cells. In future studies, we will further investigate the effect of Val on normal cells to more fully understand its mechanism of action. In addition, we have not currently conducted antitumor experiments on Val *in vivo*. However, we have noted that other researchers have experimented with the drug *in vivo* in other tumor types with some encouraging results [53]. These experimental results suggest that the drug has the potential to inhibit tumor growth. In the future, we will validate our results in an *in vivo* model to evaluate the efficacy and safety of Val against GC.

Acknowledgement: We thank LetPub (www.letpub.com) for its linguistic assistance during the preparation of this manuscript.

Funding Statement: This research was funded by Central Government Supports Local College Reform and Development Fund Talent Training Project (No. 2020GSP16), Heilongjiang Province Key Research and Development Plan Guidance Project (No. GZ20220039), Heilongjiang Touyan Innovation Team Program (No. 2019HTY078), Program of Heilongjiang Bayi Agricultural University (No. XDB201818) and Postgraduate Innovative Research Project of Heilongjiang Bayi Agricultural University (No. YJSCX2022-Y55).

Author Contributions: The authors confirm contribution to the paper as follows: study conception and design: Jinglong Cao, Shumei Li, and Tong Zhang; draft manuscript preparation: Jinglong Cao; data collection: Jinglong Cao and Jian Liu; analysis and interpretation of results: Wenshuang Hou and Anqi Wang; revised the final draft: Chang Wang

and Chenghao Jin. All authors reviewed the results and approved the final version of the manuscript.

Availability of Data and Materials: The datasets generated during analyzed study are available from the corresponding author on reasonable request.

Ethics Approval: Not applicable.

Conflicts of Interest: The authors declare that they have no conflicts of interest to report regarding the present study.

References

1. Smyth EC, Nilsson M, Grabsch HI, Grieken NC, Lordick F. Gastric cancer. Lancet. 2020;396:635–48. doi:10.1016/S0140-6736(20)31288-5.
2. Karimi P, Islami F, Anandasabapathy S, Freedman ND, Kamangar F. Gastric cancer: descriptive epidemiology, risk factors, screening, and prevention. Cancer Epidem Biomark Prev. 2014;23:700–13. doi:10.1158/1055-9965.EPI-13-1057.
3. Alterio D, Marvaso G, Ferrari A, Volpe S, Orecchia R, Jereczek-Fossa BA. Modern radiotherapy for head and neck cancer. Semin Oncol. 2019;46:233–45. doi:10.1053/j.seminoncol.2019.07.002.
4. Yoon CI, Hwang J, Kim D, Ji JH, Li JH, Lee J, et al. Prognostic impact of radiotherapy-induced-lymphopenia in patients treated with breast-conservative surgery. Nat Rev Clin Oncol. 2023;13:14372. doi:10.1038/s41598-023-41301-3.
5. Wei G, Wang Y, Yang G, Wang Y, Ju R. Recent progress in nanomedicine for enhanced cancer chemotherapy. Theranostics. 2021;11(13):6370–92. doi:10.7150/thno.57828.
6. Ziemska J, Szynal T, Mazanska M, Solecka J. Natural medicinal resources and their therapeutic applications. Roczniki Panstwowego Zakladu Higieny. 2019;70:407–13. doi:10.32394/rpzh/2019.0093.
7. Xiang Y, Guo Z, Zhu P, Chen J, Huang Y. Traditional Chinese medicine as a cancer treatment: modern perspectives of ancient but advanced science. Cancer Med. 2019;8(5):1958–75. doi:10.1002/cam4.2108.
8. Orhan IE. A review focused on molecular mechanisms of anxiolytic effect of Valerina officinalis L. in connection with its phytochemistry through *in vitro*/*in vivo* studies. Curr Pharm Design. 2021;27:3084–90. doi:10.2174/1381612827666210119105254.
9. Nawrot J, Gornowicz-Porowska J, Budzianowski J, Nowak G, Schroeder G, Kurczewska J. Medicinal herbs in the relief of neurological, cardiovascular, and respiratory symptoms after COVID-19 infection a literature review. Cells. 2022;11(12):1897. doi:10.3390/cells11121897.
10. Chen L, Feng D, Qian Y, Cheng X, Song H, Qian Y, et al. Valtrate as a novel therapeutic agent exhibits potent anti-pancreatic cancer activity by inhibiting Stat3 signaling. Phytomed. 2021;85:153537. doi:10.1016/j.phymed.2021.153537.
11. Tian S, Wang Z, Wu Z, Wei Y, Yang B, Lou S. Valtrate from Valeriana jatamansi Jones induces apoptosis and inhibits migration of human breast cancer cells *in vitro*. Nat Prod Res. 2020;34:2660–3. doi:10.1080/14786419.2018.1548454.
12. Li X, Chen T, Lin S, Zhao J, Chen P, Ba Q, et al. Valeriana jatamansi constituent IVHD-valtrate as a novel therapeutic agent to human ovarian cancer: *in vitro* and *in vivo* activities and mechanisms. Curr Cancer Drug Targets. 2013;13(4):472–83. doi:10.2174/1568009611313040009.
13. Wong RS. Apoptosis in cancer: from pathogenesis to treatment. J Exp Clin Canc Res. 2011;30(1):87. doi:10.1186/1756-9966-30-87.
14. Wu H, Chen L, Zhu F, Han X, Sun L, Chen K. The cytotoxicity effect of resveratrol: cell cycle arrest and induced apoptosis of breast cancer 4T1 cells. Toxins. 2019;11:731–11120731. doi:10.3390/toxins11120731.
15. Yang WQ, Shao F, Wang JX, Shen T, Zhao Y, Fu XY, et al. Ethyl acetate extract from Artemisia argyi prevents liver damage in ConA-induced immunological liver injury mice via Bax/Bcl-2 and TLR4/MyD88/NF-κB signaling pathways. Mol. 2022;27:7883. doi:10.3390/molecules27227883.
16. Rajabi S, Maresca M, Yumashev AV, Choopani R, Hajimehdipoor H. The most competent plant-derived natural products for targeting apoptosis in cancer therapy. Biomol. 2021;11(4):534. doi:10.3390/biom11040534.
17. Luo Y, Ma J, Lu W. The significance of mitochondrial dysfunction in cancer. Int J Mol Sci. 2020;21(16):5598. doi:10.3390/ijms21165598.
18. Lalier L, Vallette F, Manon S. Bcl-2 family members and the mitochondrial import machineries: the roads to death. Biomol. 2022;12(2):162. doi:10.3390/biom12020162.
19. Sekar G, Ojoawo A, Moldoveanu T. Protein-protein and protein-lipid interactions of pore-forming BCL-2 family proteins in apoptosis initiation. Biochem Soc Trans. 2022;50(3):1091–1103. doi:10.1042/BST20220323.
20. Zhang X, Ge YL, Zhang SP, Yan P, Tian RH. Downregulation of KDR expression induces apoptosis in breast cancer cells. Cell Mol Biol Lett. 2014;19(4):527–41. doi:10.2478/s11658-014-0210-8.
21. Agidigbi TS, Kim C. Reactive oxygen species in osteoclast differentiation and possible pharmaceutical targets of ROS-mediated osteoclast diseases. Int J Mol Sci. 2019;20:3576. doi:10.3390/ijms20143576.
22. Xu F, Xu J, Xiong X, Deng Y. Salidroside inhibits MAPK, NF- κB, and STAT3 pathways in psoriasis-associated oxidative stress via SIRT1 activation. Redox Rep. 2019;24(1):70–4. doi:10.1080/13510002.2019.1658377.
23. Lin XM, Liu SB, Luo YH, Xu WT, Zhang Y, Zhang T, et al. 10-HDA induces ROS-mediated apoptosis in A549 human lung cancer cells by regulating the MAPK, STAT3, NF-κB, and TGF-β1 signaling pathways. Evid-Based Complement Altern Med. 2020;2020:3042636. doi:10.1155/2020/3042636.
24. Lee S, Rauch J, Kolch W. Targeting MAPK signaling in cancer: mechanisms of drug resistance and sensitivity. Int J Mol Sci. 2020;21:1102. doi:10.3390/ijms21031102.
25. Ma JH, Qin L, Li X. Role of STAT3 signaling pathway in breast cancer. Cell Commun Signal. 2020;18:33. doi:10.1186/s12964-020-0527-z.
26. Patel M, Horgan PG, McMillan DC, Edwards J. NF-κB pathways in the development and progression of colorectal cancer. Transl Res. 2018;197:43–56. doi:10.1016/j.trsl.2018.02.002.
27. Kuczler MD, Olseen AM, Pienta KJ, Amend SR. ROS-induced cell cycle arrest as a mechanism of resistance in polyaneuploid cancer cells (PACCs). Prog Biophys Mol Biol. 2021;165(2):3–7. doi:10.1016/j.pbiomolbio.2021.05.002.
28. Lee W, Song G, Bae H. Laminarin attenuates ROS-mediated cell migration and invasiveness through mitochondrial dysfunction in pancreatic cancer cells. Antioxid. 2022;11(9):1714. doi:10.3390/antiox11091714.
29. Mens MMJ, Ghanbari M. Cell cycle regulation of stem cells by MicroRNAs. Stem Cell Rev Rep. 2018;14(3):309–22. doi:10.1007/s12015-018-9808-y.

30. Wang Z. Regulation of cell cycle progression by growth factor-induced cell signaling. Cells. 2021;10(12):3327. doi:10.3390/cells10123327.
31. Icard P, Fournel L, Wu Z, Alifano M, Lincet H. Interconnection between metabolism and cell cycle in cancer. Trends Biochem Sci. 2019;44(6):490–501. doi:10.1016/j.tibs.2018.12.007.
32. Tewari D, Patni P, Bishayee A, Sah AN, Bishayee A. Natural products targeting the PI3K-Akt-mTOR signaling pathway in cancer: a novel therapeutic strategy. Semin Cancer Biol. 2022;80:1–17. doi:10.1016/j.semcancer.2019.
33. Li E, Gao Y, Mou L, Zhang Z. Anticancer activity of Germacrone terpenoid in human osteosarcoma cells is mediated via autophagy induction, cell cycle disruption, downregulating the cell cycle regulatory protein expressions and cell migration inhibition. Acta Biochim Pol. 2022;69:305–8. doi:10.18388/abp.2020_5712.
34. Janiszewska M, Primi MC, Izard T. Cell adhesion in cancer: beyond the migration of single cells. J Biol Chem. 2020;295:2495–505. doi:10.1074/jbc.
35. Scarpa M, Singh P, Bailey CM, Lee JK, Kapoor S, Lapidus RG, et al. PP2A- activating drugs enhance FLT3 inhibitor efficacy through AKT inhibition-dependent GSK-3β-mediated c-Myc and Pim-1 proteasomal degradation. Mol Cancer Ther. 2021;20(4):676–90. doi:10.1158/1535-7163.MCT-20-0663.
36. Xu X, Zou L, Yao Q, Zhang Y, Gan L, Tang L. Silencing DEK downregulates cervical cancer tumorigenesis and metastasis via the DEK/p-Ser9-GSK-3β/p-Tyr216-GSK-3β/β-catenin axis. Oncol Rep. 2017;38:1035–42. doi:10.3892/or.2017.5721.
37. Sethy C, Kundu CN. 5-Fluorouracil (5-FU) resistance and the new strategy to enhance the sensitivity against cancer: implication of DNA repair inhibition. Biomed Pharmacother. 2021;137:111285. doi:10.1016/j.biopha.2021.111285.
38. Shafabakhsh R, Asemi Z. Quercetin: a natural compound for ovarian cancer treatment. J Ovarian Res. 2019;12(1):55. doi:10.1186/s13048-019-0530-4.
39. Yang Z, Zhang Q, Yu L, Zhu J, Cao Y, Gao X. The signaling pathways and targets of traditional Chinese medicine and natural medicine in triple-negative breast cancer. J Ethnopharmacol. 2021;264:113249. doi:10.1016/j.jep.2020.113249.
40. Ślefarska-Wolak D, Heinzle C, Leiherer A, Ager C, Muendlein A, Mezmale L, et al. Volatilomic signatures of AGS and SNU-1 gastric cancer cell lines. Mol. 2022;27:4012. doi:10.3390/molecules27134012.
41. Carneiro BA, El-Deiry WS. Targeting apoptosis in cancer therapy. Nat Rev Clin Oncol. 2020;17(7):395–417. doi:10.1038/s41571-020-0341-y.
42. Mehrbod P, Ande SR, Alizadeh J, Rahimizadeh S, Shariati A, Malek H, et al. The roles of apoptosis, autophagy and unfolded protein response in arbovirus, influenza virus, and HIV infections. Virulence. 2019;10(1):376–413. doi:10.1080/21505594.2019.1605803.
43. Ribeiro DL, Tuttis K, de Oliveira LCB, Serpeloni JM, Gomes INF, Lengert AVH, et al. The antitumoral/antimetastatic action of the flavonoid brachydin a in metastatic prostate tumor spheroids *in vitro* is mediated by (Parthanatos) PARP-related cell death. Pharmaceutics. 2022;14(5):963. doi:10.3390/pharmaceutics14050963.
44. Qin LG, Cao X, Kaneko T, Liu XG, Wang GP, Li SSC. Dynamic interplay of two molecular switches enabled by the MEK1/2-ERK1/2 and IL-6-STAT3 signaling axes controls epithelial cell migration in response to growth factors. J Biol Chem. 2021;297(4):101161. doi:10.1016/j.jbc.2021.101161.
45. Steyn PJ, Dzobo K, Smith RI, Myburgh KH. Interleukin-6 induces myogenic differentiation via JAK2-STAT3 signaling in mouse C2C12 myoblast cell line and primary human myoblasts. Int J Mol Sci. 2019;24(21):273. doi:10.3390/ijms20215273.
46. Chen X, Zhao Y, Luo W, Chen S, Lin F, Zhang X, et al. Celastrol induces ROS-mediated apoptosis via directly targeting peroxiredoxin-2 in gastric cancer cells. Theranostics. 2020;10(22):10290–308. doi:10.7150/thno.46728.
47. Guo R, Chen X, Nguyen T, Chai J, Gao Y, Wu J, et al. The strong anti-tumor effect of Smp24 in lung adenocarcinoma A549 cells depends on its induction of mitochondrial dysfunctions and ROS accumulation. Toxins. 2022;14(9):590. doi:10.3390/toxins14090590.
48. Liu N, Wang KS, Qi M, Zhou YJ, Zeng GY, Tao J, et al. Vitexin compound 1, a novel extraction from a Chinese herb, suppresses melanoma cell growth through DNA damage by increasing ROS levels. J Exp Clin Canc Res. 2018;37(1):269. doi:10.1186/s13046-018-0897-x.
49. Chang PR, Liou JW, Chen PY, Gao WY, Wu CL, Wu MJ, et al. The neuroprotective effects of flavonoid fisetin against corticosterone-induced cell death through modulation of ERK, p38, and PI3K/Akt/FOXO3a-dependent pathways in PC12 cells. Pharmaceutics. 2023;15(10):2376. doi:10.3390/pharmaceutics15102376.
50. Guo Z, Guo ZH, Wang H, Li Z, Liu N. Ampelopsin inhibits human glioma through inducing apoptosis and autophagy dependent on ROS generation and JNK pathway. Biomed Pharmacother. 2019;116:108524. doi:10.1016/j.biopha.2018.12.136.
51. Sun Y, Liu Y, Ma X, Hu H. The influence of cell cycle regulation on chemotherapy. Int J Mol Sci. 2021;22:6923. doi:10.3390/ijms22136923.
52. Swaffer MP, Jones AW, Flynn HR, Snijders AP, Nurse P. CDK substrate phosphorylation and ordering the cell cycle. Cell. 2016;167(7):1750–61. doi:10.1016/j.cell.2016.11.034.
53. Liu Z, Zhu Q, Song E, Song Y. Polybrominated diphenyl ethers quinone exhibits neurotoxicity by inducing DNA damage, cell cycle arrest, apoptosis and p53-driven adaptive response in microglia BV2 cells. Toxicol. 2021;457(445–459):152807. doi:10.1016/j.tox.2021.152807.
54. Shannan B, Seifert M, Boothman DA, Tilgen W, Reichrath J. Clusterin and DNA repair: a new function in cancer for a key player in apoptosis and cell cycle control. J Mol Histol. 2006;37:183–8. doi:10.1007/s10735-006-9052-7.
55. Wengner AM, Siemeister G, Lücking U, Lefranc J, Wortmann L, Lienau P, et al. The novel ATR inhibitor BAY 1895344 is efficacious as monotherapy and combined with DNA damage-inducing or repair-compromising therapies in preclinical cancer models. Mol Cancer Ther. 2020;19(1):26–38. doi:10.1158/1535-7163.MCT-19-0019.
56. Zhang W, Liu C, Li J, Lu Y, Li H, Zhuang J, et al. Tanshinone IIA: new perspective on the anti-tumor mechanism of a traditional natural medicine. Am J Chinese Med. 2022;50:209–39. doi:10.1142/S0192415X22500070.